



Universidad Autónoma  
de Madrid

**Biblos-e Archivo**  
Repositorio Institucional UAM

**Repositorio Institucional de la Universidad Autónoma de Madrid**

<https://repositorio.uam.es>

Esta es la **versión de autor** del artículo publicado en:  
This is an **author produced version** of a paper published in:

*Organic and Biomolecular Chemistry* 18.17 (2020): 3334-3345

**DOI:** <https://doi.org/10.1039/D0OB00529K>

**Copyright:** © 2020 The Royal Society of Chemistry

El acceso a la versión del editor puede requerir la suscripción del recurso

Access to the published version may require subscription

# The quasi-irreversible inactivation of Cytochrome P450 enzymes by paroxetine: A computational approach

Emadeldin M. Kamel <sup>\*,[a], [b]</sup> and Al Mokhtar Lamsabhi <sup>[a], [c]</sup>

[a] Dr. E. Kamel and Prof. Dr. A. Lamsabhi  
Departamento de Química  
Universidad Autónoma de Madrid  
Módulo 13 Campus de Excelencia UAM-CSIC Cantoblanco, Madrid, Spain  
E-mail: [emad.abdelhameed@sceince.bsu.edu.eg](mailto:emad.abdelhameed@sceince.bsu.edu.eg)  
[mokhtar.lamsabhi@uam.es](mailto:mokhtar.lamsabhi@uam.es)

[b] Dr. E. Kamel  
Chemistry Department  
Faculty of Science, Beni-Suef University  
Beni-Suef, 62514, Egypt.

[c] Prof. Dr. A. Lamsabhi  
Institute for Advanced Research in Chemical Sciences (IAdChem)  
Universidad Autónoma de Madrid  
28049 Madrid, Spain

**Abstract:** DFT calculations were employed to explore the mechanism-based inactivation (MBI) of P450 with the paroxetine. The drug-enzyme interactions were figured out through studying energy profiles of three competitive mechanisms. Our DFT analysis revealed that, paroxetine is a potent P450's inhibitor because of the availability of two active sites for the MBI. The inactivation of P450 at secondary amine active site of paroxetine was found to be mainly via hydrogen atom transfer (HAT) pathway because of the lower energy demand of its rate determining step. Our comparative investigation showed that, LS state is the predominant route in the MBI of P450 by paroxetine at the methylene dioxo active site as a result of being rebound barrier-free mechanism. The results of docking analysis are coincided with the outputs of DFT calculations since the docking pose with the lowest binding affinity is that for conformation with polar interaction between amino group of paroxetine and the oxo moiety of P450's active site. Also, the binding between paroxetine and the enzyme was shown to be likely to occur by the formation of polar bonds, hydrophobic interactions and  $\pi$ - $\pi$  interactions. Assessment of the molecular dynamics (MD) simulations trajectories revealed the favorable interaction of paroxetine with P450.

## Introduction

Cytochrome P450 (P450) heme-thiolate enzymes are predominantly liver-localized enzymes that are responsible for the catalyzed biotransformation of drugs and xenobiotics [1]. The biological functions of P450s, such as detoxification and reactive metabolites formation, are mainly due to their ability to catalyze and insert oxygen into large number of substrates [2]. Consequently, studying such catalyzed biotransformation might attract technological applications in many aspects as chemical and pharmaceutical industries [3].

P450 enzymes are known for their oxidative influence on aryl, amino and alkyl methylenedioxy compounds [4]. The catalytic cycle of P450 is usually initiated by the displacement of the distal water ligand followed by the binding of the substrate [5]. In this catalytic cycle, three steps are more prone to inhibition namely: (i) substrate binding, (ii) molecular oxygen binding after the first electron transfer and (iii) the actual catalytic oxidation of substrate [6]. According to mechanism of inhibition, P450 inhibitors can be subdivided into three different categories: (1) Reversible binding inhibitors, which interfere in the catalytic cycle before the substrate is actually oxidized, these inhibitors are broadly reversible competitive or noncompetitive [7], (2) Quasi-irreversible complexes forming inhibitors, those that function during or after the oxygen transfer step, and form complexes with the heme iron

atom so they are counted in the class of mechanism-based inactivators [7], and (3) Irreversible binding inhibitors, that bind to the protein or heme moiety, so they speed up the oxidative degradation of the prosthetic heme [7].

Inhibition of P450 via mechanism-based inactivation (MBI) is basically not a favorable process, since it has an adverse influence on the catalyzed biotransformation processes. However, MBI of P450 is beneficial in increasing the probability of attaining higher degree of selectivity when a specific P450 is targeted [6a, 7c, 8]. The formation of covalent adduct after the catalyzed biotransformation of inhibitors into reactive metabolites is the main cause for this high selectivity [9].

Paroxetine, commonly known as Paxil and Seroxat among others, is a very potent inhibitor of P450 [11]. Paroxetine is an antidepressant of selective serotonin reuptake inhibitors (SSRIs) family [12]. Paroxetine is eliminated by extensive hepatic catalyzed biotransformation, involving P450's enzymatic system, and it is usually oxidized to inactive metabolites [13]. Effectively and efficiently, paroxetine is used as a pretreatment to inhibit the metabolism of tramadol to its active metabolite via inactivating P450. However, it doesn't set aside the hypoalgesic effect of tramadol in human experimental pain models [12].

A precise understanding of P450-drug interaction by *in silico* analysis would afford more reliable predictions for the MBI of P450 than those already figured out [10]. Docking and Molecular dynamics (MD) are *in-silico* techniques that model particles interactions in a system with initially specified parameters. MD techniques have been employed by many investigators to find out information about the drug-enzyme interactions and reactivities [14]. Even though large number of studies reported the MD simulations of P450s, the mechanisms-based drug entry and binding into the active site of P450 is still a matter of debate. X-ray analysis and MD simulations have provided worthy information about the structural characteristics and variations in these interactions [15]. In P450 enzymes, the active site is deeply submerged into the protein and separated from the bulk solvent. Thus, MD simulations is crucial to identify entry and binding sites of the drug into the active site cavity [16]. Also, exploring the structural nature and mechanism of action of P450 by MD simulations would provide valuable information for designing new optimal drugs to act as potent P450's inhibitors and activators.

In this work, a quantum chemical study was reported to explore the mechanism-based inactivation of P450 by paroxetine. Two conceivable active sites on paroxetine for the paroxetine-P450's interaction, namely; methylenedioxy and the secondary amine group. Consequently, two suggested pathways for the inactivation of P450 by paroxetine; the C-H hydroxylation at the methylenedioxy site and N-H hydroxylation, the latter may proceed via OAR or HAT. These mechanisms were subjected to

extensive DFT studies to understand the mechanistic details associated with the inactivation of P450 by paroxetine and to determine the thermodynamically favorable reaction route. Also, docking and MD simulations techniques were utilized to perceive the structural basis of paroxetine-P450 interactions and the influence of paroxetine on the conformation of the enzyme.

## Results and Discussion

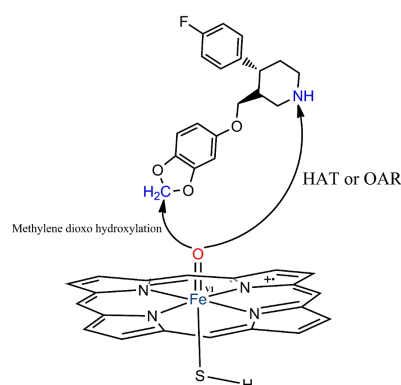
### Active site for Paroxetine

From the chemical point of view the chemical reactive sites of paroxetine can easily deduced from the difference of polarity of its atoms. However, in order to get a realistic approach to the biological environment that might be involved in their interaction we choose docking paroxetine onto the binding site of the P450. After many attempts the best docking pose for the ligand was selected according to its conformation and docking energy. The low binding affinity (-8.7 kcal/mol) suggests the formation of a stable paroxetine-P450 complex. The applied docking grid box was set at 30 x 30 x 30 (x,y,z) and the binding site residues were Arg108, Ser209, Phe100, Phe114, Phe476, Leu361, Leu362, Leu366, Val292, Thr301, Thr304, Ile205, Glu300 and Val479. There were three hydrogen bonding interactions between paroxetine and the enzyme (Figure 4) because of the availability of polar hydrogens in the inhibitor structure. The availability of  $\pi$ - $\pi$  interactions between aromatic species is a leading factor in molecular recognition and plays a crucial role in adapting the conformation of paroxetine in the binding pocket of the enzyme. The results of docking analysis of paroxetine-P450 complex showed three phenylalanine residues at the binding site; Phe100, Phe114 and Phe476. These residues have the ability to create electrostatically favorable  $\pi$ - $\pi$  interactions that could possibly interact with the aromatic rings of the inhibitor. This is confirmed by the fact that paroxetine interacts with phenylalanine residues by the electrostatically attractive interaction edge-to-face and offset stacked orientation types rather than the unfavorable face-to-face and edge-to-edge orientations [32]. It is interesting to note that the best docking pose is that conformation with the polar bond between the secondary amine and the oxo moiety of P450's active site which might direct our DFT calculations. The results of molecular docking analysis bring to light the fact that interaction between paroxetine and the enzyme is predominant by the formation of polar bonds and  $\pi$ - $\pi$  interactions. Also, these outputs shed the light on the contribution of not only active sites (methylenedioxy and amino) but also aromatic rings in paroxetine structure in the MBI of P450 by the electrostatically favored  $\pi$ - $\pi$  interactions. The surface representation of free P450 and paroxetine bound to the internal cavity of P450 is shown in Figure 5. Generally, molecular docking analysis confirms the potency of paroxetine as P450 inhibitor.

### Hydroxylation of P450.

Localized the site of action of paroxetine the inhibition of the enzyme might occur in different ways. Let's first recover the state of works done computationally on the P450's reaction mechanism. Previously reported theoretical studies on P450's active site concerned mainly C-H hydroxylation [17], C=C epoxidation [18] and heteroatoms oxidation [19]. C-H bond hydroxylation, catalyzed by P450, is revealed as an important metabolic process in detoxifying toxic and endogenous materials [6a]. These mechanisms were subjected to intensive investigations, nevertheless, its characteristics are still a matter of debate. Generally, this mechanism was agreed to proceed via an initial hydrogen abstraction from the C-H bond by means of compound I (Cpd I), that was modeled by ferryl-oxene ( $\text{Por}^{+}\text{FeO}$ ) species with  $\text{HS}^{-}$  as a proximal ligand and stands for P450's active site [17b, 20]. Subsequently, the alkyl radical rebound to the oxygen of the

hydroxy ferryl species generating ferryl-hydroxylated C-H complex, then the alcohol is released and the P450's resting state is retrieved by coordinating to the water ligand [17b, 20]. In human, secondary amine xenobiotics is catalytically metabolized by P450s leading to the formation of hydroxylamines [21]. So far, four mechanisms are conceivable for the N-hydroxylation of secondary alkylamines; hydrogen atom transfer (HAT), oxygen addition rearrangement (OAR), single-electron transfer (SET) and proton transfer (PT) [22]. In HAT mechanism, H-atom is abstracted from the nitrogen of the amine to the oxygen of the ferryl oxo center and subsequently, a rebound of the alkyl radical to the oxygen of the iron-hydroxyl species yielding hydroxylamine  $\text{ArNHOH}$  [23]. While in OAR mechanism, the N-oxide obtained from the addition of FeO oxygen to N of the amine rearranges to N-hydroxylamine [23]. A single electron is transferred in the SET mechanism from the amine to the FeO followed by proton transfer and finally the amine radical rebound to the ferric hydroxy species [24]. This intermediate amine radical could undergo a two-electron transfer (TET) process to afford an aminyl cation [23]. In the proton transfer mechanism (PT), a proton is transferred from the amine to  $\text{FeOO}^{2-}$  to form the ferric hydroperoxide anion  $\text{FeOOH}^{-}$  [24].



Scheme 1. Model for our DFT calculations for the conceivable pathways for paroxetine-P450 interactions.

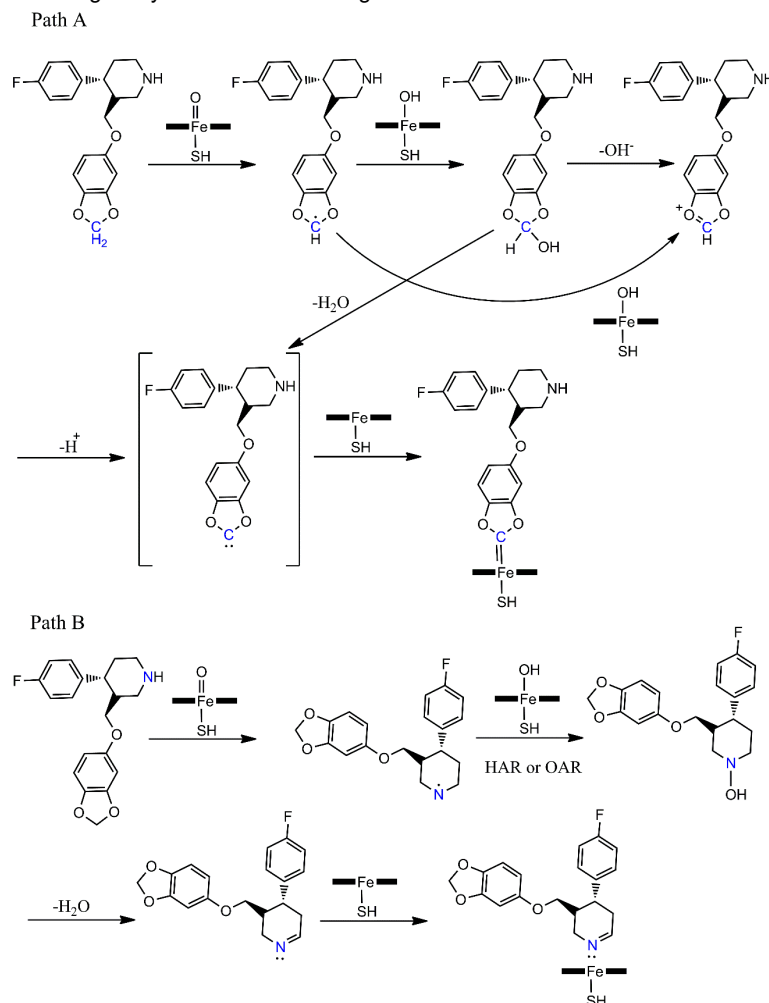
Generally, P450 mechanisms involve two-state reactivity (TSR) nascent from the two degenerate ground states of Cpd I that was modeled by ferryl-oxene ( $\text{Por}^{+}\text{FeO}$ ) species with  $\text{HS}^{-}$  as a proximal ligand, the TSR are low-spin (LS, doublet) and high-spin (HS, quartet) [17b, 25]. The TSR hypothesis assumes a competition between two comparable reaction routes, and the prevailing pathway is substrate and environmental dependent [26]. A perfect C-H hydroxylation mechanism exposes a doubled reaction route because of the HS and LS states, these two paths remain energetically adjacent in the H-abstraction stage then bifurcate during the rebound step [6a]. In this mechanism, the quartet state route shows a significant rebound transition state energy barrier while the LS state pathway is concerted with insignificant radical intermediate lifetime [19c, 27]. The situation in case of hydroxylation of alkylamines is a bit more complicated because of the presence of two competitive reaction routes; HAT and OAR. Where a slight energetic preference for the HAT was detected, and the highest transition state energy barrier was observed for both LS and HS states [19b]. Nevertheless, in another study the two paths were most likely to occur. On the contrary to the previously reported, the rearrangement step in the OAR mechanism was shown to pass through a higher energy barrier, and that for the HAT mechanism the rebound step process via barrier-free mode in the LS state [23].

In the present study the choice of paroxetine tries to recover the different possibilities discussed above and so the three mentioned mechanisms: The C-H hydroxylation where MBI mechanism is involved and N-H hydroxylation where both HAT and OAR pathways are expected. The probability of both processes to take place is similar since the binding energy of paroxetine with Cpd I through C-H bond is slightly inferior than the interaction with its N-H group. In fact, the energy involved in the former is about -1.5

whereas in the later is about -2.05 kcal/mol at the higher level of theory. The mechanisms of P450 are susceptible to follow different routes to throw off water molecule. Our computational efforts were carried out to recover all these possibilities. Different pathways for the MBI of P450 by paroxetine were assessed by setting up a model for the possible active sites of the P450-paroxetine interaction (Scheme 1). Two possible pathways, Paths A and B, for the MBI of P450 by paroxetine were examined, which were discriminated by the paroxetine's active site attacked by the oxo ferryl moiety of P450 (scheme 2). In path A, the catalyzed biotransformation process is mainly proceeding via C-H hydroxylation of the methylene dioxy moiety of paroxetine (scheme 3), while in path B the N-hydroxylation of the secondary amine is the main route responsible for the MBI of P450. Consequently, the four mechanisms underlying the N-hydroxylation by P450 have been discussed (scheme 4) [23-24]. Figures 1 and 2 show the obtained energy profiles (in kcal/mol) and key geometric features at the UB3LYP/B2//B1+ZPE(B1) and UB3LYP (SCRF)/B2//B1+ZPE(B1) levels for both the doublet and quartet states of The MBI of P450 by paroxetine at methylene dioxy and secondary amine active sites of paroxetine, respectively.

**Methylen Hydroxylation (path A):** Initially, the energy of the reactant complex ( $^{2,4}\text{RC}_m$ ) in both doublet and quartet states is stabilized by a weak hydrogen bonding interaction between a hydrogen atom at the methylene dioxy active site of paroxetine and the oxo moiety of the ferryl oxo species. In this stage the LS and HS states are degenerated with a negligible energy difference, about 0.08 kcal/mol. The process begins by the rate determining

step for both LS and HS pathways in which the hydrogen atom is transferred from methylene dioxy of paroxetine to the  $\text{Fe}^{\text{IV}}=\text{O}$  of Cpd I ( $^{2,4}\text{TS-Hm}$ ). The energy barrier of the quartet H-abstraction transition state ( $^4\text{TS-Hm}$ ) is higher than its doublet parallel ( $^2\text{TS-Hm}$ ) by  $\approx 1.7$  kcal mol $^{-1}$ , this discrimination could be noticed from the variation of the arrangement  $\text{O}\cdots\text{H}\cdots\text{C}$  bond distances in both LS and HS states. Moreover, the two transition states,  $^{2,4}\text{TS-Hm}$ , possess the geometrical features of H-abstraction transition states with a nearly collinear arrangement of the  $\text{O}\cdots\text{H}\cdots\text{C}$  moiety ( $\text{O}\cdots\text{H}\cdots\text{C}$  bond angles of  $170.5\text{--}175^\circ$ ) [17b, 28]. It should be mentioned that, most of the structural characteristics of H-abstraction transitions states are included, including shortening of the Fe-S bond length, lengthening of the Fe-O bond length, light breathing of the porphyrin, a semi resting of iron into the porphyrin plane and the corresponding imaginary frequency [17b, 24]. As previously reported, the LS and HS H-abstraction energy barriers of paroxetine-P450 interaction are not discriminated because this reaction is governed by TSR principle [6a, 17b]. Subsequently, a radical intermediate ( $^{2,4}\text{INT}_m$ ) is formed after the H-abstraction from paroxetine to the ferryl oxo species, this intermediate is a complex of the paroxetine methylene dioxy radical with  $\text{FeOH}(\text{PorSH})$ . In this complex, the  $\text{CH}^\bullet$  of paroxetine is still connected to the OH group of the ferryl hydroxy porphyrin [28a]. As expected, the LS state ( $^2\text{INT}_m$ ) is slightly lower than its HS counterpart ( $^4\text{INT}_m$ ) by energy difference less than 0.5 kcal mol $^{-1}$  which confirm the proceeding of this reaction via TSR as previously mentioned.

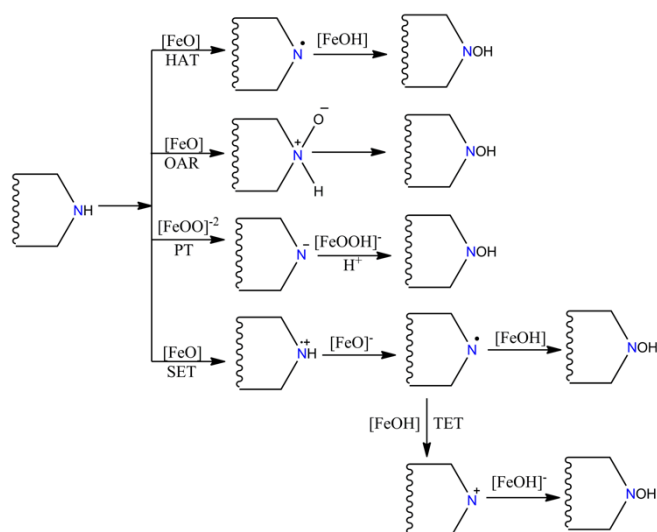
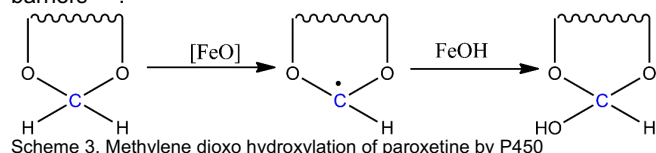


Scheme 2. The general mechanisms for the quasi-irreversible inactivation of P450 enzymes by paroxetine at the two conceivable active sites; Path A: methylene dioxy hydroxylation; Path B: N-hydroxylation of the secondary amine.

After radical intermediate complexes formation ( $^{2,4}\text{INT}_\text{m}$ ), a rebound reaction occurs for these intermediates to complete its catalytic transformation. This reaction involves the rebound of these intermediates to OH of ferryl hydroxy species to form hydroxylated paroxetine within methylene dioxo active site ( $^{2,4}\text{P-OH}_\text{m}$ ) and  $\text{Fe}(\text{PorSH})$ . It is apparent that, the LS rebound process proceeds via energy barrier-free mode (concerted mechanism), while the HS pathway involves a two-step process with considerable rebound energy barrier as previously reported for C-H hydroxylation [17b, 29]. These variations in kinetics between HS and LS reaction pathways assume that C-H hydroxylation of paroxetine at the methylene dioxo active site is superior for the LS route over its HS counterpart.

**Amine hydroxylation (path B):** the reaction energy profile for HAT and OAR routes for the MBI of paroxetine-p450's interaction along with the geometrical features are represented in figure 2. The HAT and OAR mechanisms are directed to right and left, respectively. Analogue to the methylene dioxo pathway, the reactant complexes in LS and HS states ( $^{2,4}\text{RC}$ ) are also stabilized by hydrogen bonding interaction between the hydrogen of the secondary amine site and the oxo center of Cpd I. In the  $^{2,4}\text{RC}$ , the formed hydrogen bond is stronger than that in case of  $^{2,4}\text{RC}_\text{m}$  ( $\text{O}\cdots\text{H}$  distance for  $^{2,4}\text{RC} \sim 2.08 \text{ \AA}$  versus  $\sim 2.2 \text{ \AA}$  for  $^{2,4}\text{RC}_\text{m}$ ), this is mainly due to the electronegativity differences between the atoms involved (nitrogen and carbon). Obviously, a quite meager H-abstraction energy barrier ( $^{2,4}\text{TS}_\text{H}$ ) in the PCM-protein imitated model for both LS and HS state of the HAT route (2.9 and 2.6 kcal mol $^{-1}$  for LS and HS, respectively) afforded radical cluster intermediate ( $^{2,4}\text{INT}_\text{H}$ ) as iron-hydroxy porphyrin species ( $\text{PorFe}^{\text{IV}}\text{OH}$ ). Oppositely, the initial oxygen addition to the nitrogen lone pair energy barriers ( $^{2,4}\text{TS}_\text{O}$ ) calculated for the OAR pathway are generally higher than those obtained for the HAT H-abstraction transition state pathway (7 and 5.7 kcal mol $^{-1}$  for LS and HS, respectively) (see figure 2). It should be noted that, the energy barriers of the first transition states for both methylene dioxo ( $^{2,4}\text{TS-H}_\text{m}$ ; 7.1 and 5.4 kcal mol $^{-1}$  for HS and LS, respectively) and OAR ( $^{2,4}\text{TS}_\text{O}$ ; 7 and 5.7 kcal mol $^{-1}$  for LS and HS, respectively) pathways are nearly equal. This observation is of particular interest since it shed the light on suggesting the same probability for initiating both mechanisms. In OAR mechanism, the formed N-oxide as an intermediate complex through O addition to N lone pair ( $^{2,4}\text{INT}_\text{O}$ ) will be mainly in the doublet state (13.8 and 15.2 kcal mol $^{-1}$  for both HS and LS, respectively) as commonly known for nitrogen oxidation [19b].

Subsequent to the secondary amino radical intermediate formation in HAT mechanism, the ferryl hydroxy moiety rebound to the amino radical to afford the hydroxylation product ( $^{2,4}\text{P-OH}$ ). Contrary to the previously reported in the literature [23], the hydroxylation product ( $\text{P-OH}$ ) in both LS and HS states is formed via significant rebound barriers with LS and HS states being degenerated. Also, the energies of rebound barriers in LS and HS states ( $^{2,4}\text{TS-reb}_\text{H}$ ) are higher than their analogues of H-abstraction transition states ( $^{2,4}\text{TS}_\text{H}$ ) in contrast to what is depicted for the C-H hydroxylation mechanisms, where the energies of the rebound barriers were permanently lower than H-abstraction barriers [30].



Scheme 4. Alternative mechanisms for the N-hydroxylation of paroxetine by P450, HAT: H atom transfer; OAR: oxygen addition rearrangement; SET: single-electron transfer; TET: two-electron transfer; PT: proton transfer.

The hydroxylation product ( $^{2,4}\text{P-OH}$ ) from the OAR route is obtained from the N-oxide intermediate ( $^{2,4}\text{INT}_\text{O}$ ) via H atom transfer from N to O. As expected, the energies of the rebound barriers in this mechanism is larger than those of the O addition step ( $^{2,4}\text{TS-reb}_\text{O}$ ;  $\sim 25$  and  $14 \text{ kcal mol}^{-1}$  for HS and LS, respectively). Accordingly, this H atom transfer step would express the overall rate determining step in the OAR pathway. It has been always depicted a relatively larger OAR rebound energy barriers for LS and HS states [31]. In contrast, our findings showed a smaller rebound barrier for the LS state ( $\sim 14 \text{ kcal mol}^{-1}$ ) than those previously reported for the N-hydroxylation [23, 31] suggesting an increased probability for OAR mechanism to take part in the catalyzed biotransformation of paroxetine. However, the OAR mechanism is still thermodynamically less favorable pathway for the N-hydroxylation mechanism of paroxetine as a result of the higher energy demand of its rate determining step than that of HAT route.

Overall, our findings for the N-hydroxylation of paroxetine assumed that, the OAR pathway cannot contend against the HAT pathway because of the higher energy requirements of the rate determining step of the former. Also, the proceeding of the OAR pathway via LS state with a rebound barrier lower than expected ( $\sim 14 \text{ kcal mol}^{-1}$ ) would suggest a better probability for the OAR route to share in the MBI of P450 by paroxetine than those previously reported for OAR pathway.

What is next after hydroxylation of paroxetine? As it is represented in scheme 2 in both scenarios, path A and path B, the final step is the lost of water molecule and the interaction of paroxetine with heme. To overcome the mechanistic of these processes, figure 3 reports the calculated energy profile (in kcal/mol) and key geometric features at the same level of theory for hydroxy paroxetine complex at the methylene dioxo and amino active sites. The obtained profile for dehydration of hydroxylated paroxetine complex in both mechanisms revealed the tendency of paroxetine to coordinate tightly to the heme iron atom. This mechanism is partially responsible for the inhibition of P450. The transition states for the hydrogen transfer from paroxetine to the added hydroxyl ( $^{2,4}\text{TS-D}_\text{m}$  for methylenedioxo mechanism and  $^{2,4}\text{TS-D}_\text{N}$  for secondary amine pathway) suggest the elimination of water from hydroxylated paroxetine complex to afford the paroxetine-heme coordinated complex ( $^{2,4}\text{P-C}_\text{m}$  and  $^{2,4}\text{P-C}_\text{N}$  for methylenedioxo and secondary amine deactivations, respectively). The change in bond distances between C-O and N-O along these pathways in both mechanisms behold a significance probability for the dehydration steps to occur. The considerable energies of transition states in both mechanisms and the close energies of reactants and products in



methylenedioxy route leads to the conclusion that the inactivation of P450 by paroxetine is a quasi-irreversible process under unique experimental conditions [4].

Our comparative study revealed the proceeding of the MBI of P450 by paroxetine at the methylene dioxy reactive site by a LS state mechanism with rebound barrier-free mode. As well, the inactivation of P450 at the amino group of paroxetine is obviously proceed through HAT pathway because of the lower energy requirements of its rate determining step. Interestingly, the nearly equal total energy demand for the inactivation of P450 by paroxetine at the methylene dioxy active (LS state,  $^2\text{TS-Hm} \sim 5.4$  kcal mol $^{-1}$ , free rebound barrier) and at the secondary amine

active site by HAT mechanism (LS or HS state,  $^2,^4\text{TS}_\text{H} \sim 2.9$  and  $2.6$  kcal mol $^{-1}$  for LS and HS, respectively;  $^2,^4\text{TS-reb}_\text{H} \sim 7$  and  $6.7$  kcal mol $^{-1}$  for LS and HS, respectively) would suggest an equal probability for both reaction to occur. This fact leads to the conclusion that paroxetine is a potent P450's inhibitor because of the presence of two reactive sites available for P450 interaction. In addition to, the increased share of OAR pathway besides HAT pathway in N-hydroxylation of paroxetine due to thermodynamically possible LS state rebound than those commonly known for OAR mechanism.

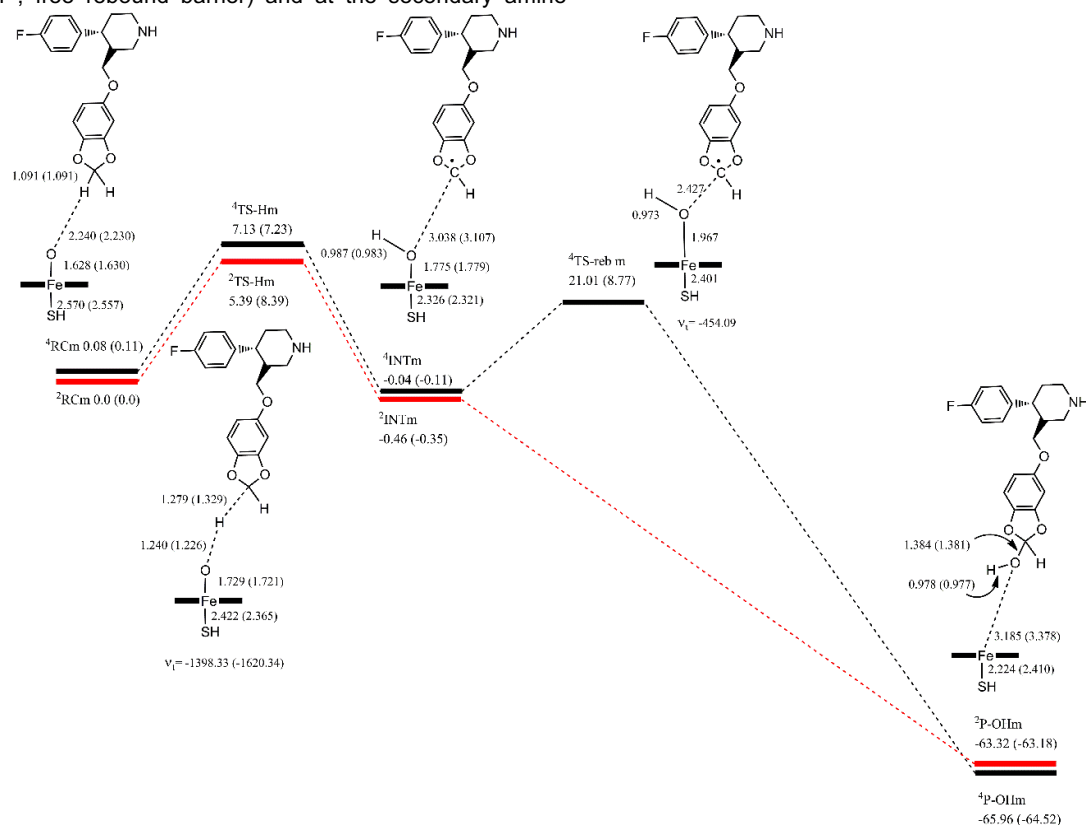


Figure 1. Energy profiles (in kcal mol $^{-1}$ ) for inactivation of P450 at the methylene dioxy active site of paroxetine calculated at the B3LYP/B2//B1+ZPE(B1) (in parentheses) and the B3LYP (SCRF)/B2//B1+ZPE(B1) levels, along with geometrical features for the reaction species in both LS and HS (in parentheses) states.

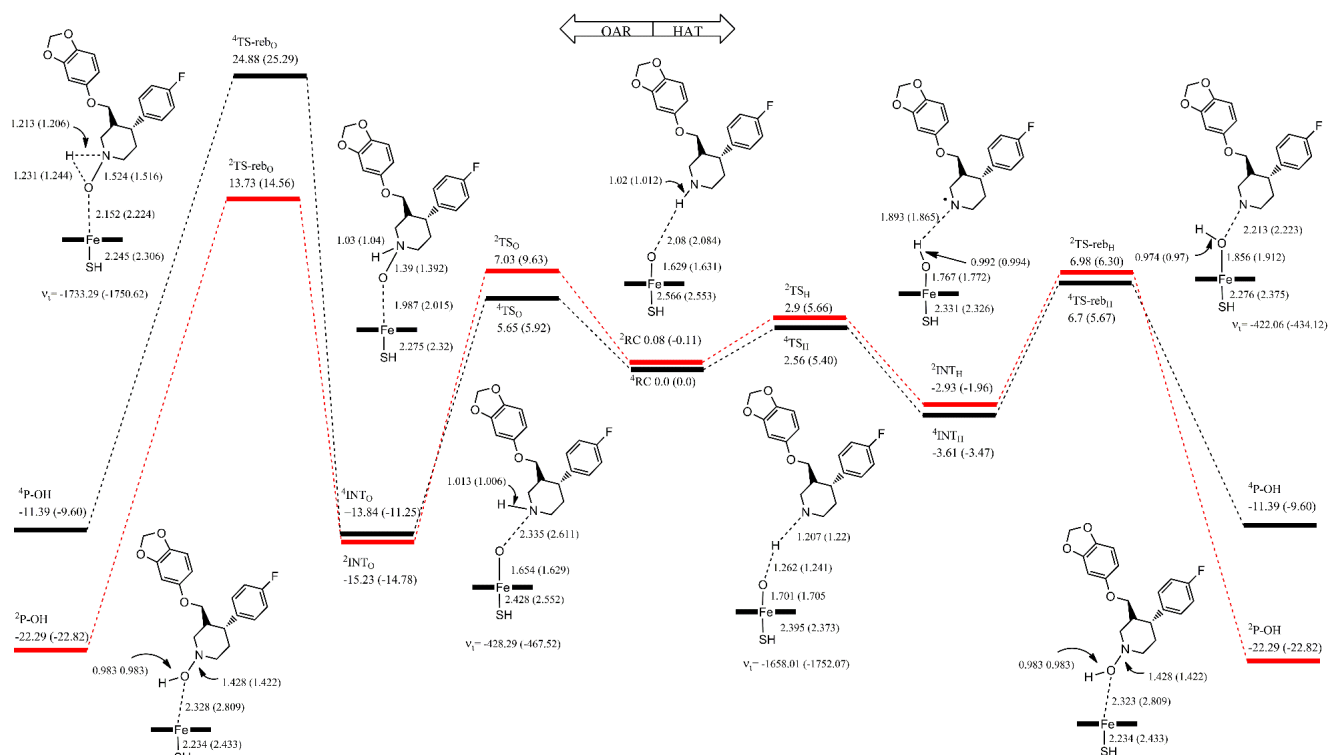


Figure 2. Energy profiles (in kcal mol<sup>-1</sup>) for inactivation of P450 at the secondary amine active site of paroxetine obtained at the B3LYP/B2//B1+ZPE(B1) (in parentheses) and the B3LYP (SCRFB2/B1+ZPE(B1) levels, along with geometrical features for the reaction species in both LS and HS (in parentheses) states.

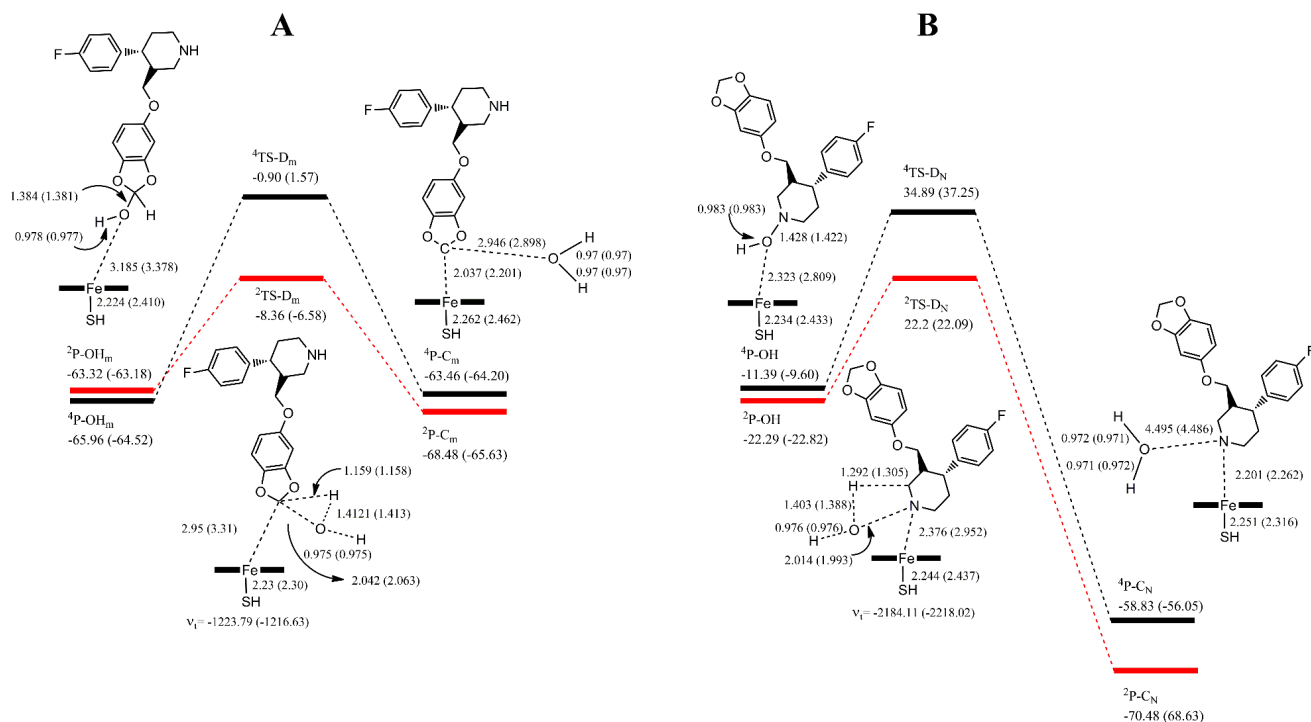


Figure 3. Energy profiles (in kcal mol<sup>-1</sup>) for the coordination of the dehydrated hydroxy paroxetine complex to the iron atom of the heme at the methylene dioxa (A) and amino (B) active sites obtained at the B3LYP/B2//B1+ZPE(B1) (in parentheses) and the B3LYP (SCRFB2/B1+ZPE(B1) levels, along with geometrical features for the reaction species in both LS and HS (in parentheses) states.

## Molecular Dynamics Simulations

To show up the stability of paroxetine in an enzyme environment, its interaction with P450 was screened by performing MD simulations for P450 and P450-paroxetine complex with intensive analysis of the MD trajectories including root mean square deviations (RMSD), hydrogen bonding profile, root mean square fluctuation (RMSF), radius of gyration ( $R_g$ ) and solvent accessible surface area (SAS).

The paroxetine interactions with the active site amino acid residues of P450 were examined during the 10 ns MD simulation through investigating the hydrogen bonding profile of protein–ligand interactions as shown in Figure 6. The hydrogen bonding profile of paroxetine-P450 complex revealed three hydrogen bonds formation behavior with two amino acids residues and the heme residue in the P450 active pocket, two H-bond is stable and the third is weaker throughout the 10 ns MD simulations.

The stability and integrity of the system (enzyme, water, ions, etc.) during the entire 10 ns MD simulations were studied by analyzing the RMSDs in water environment of the backbone atoms of P450 as a function of time for the protein and paroxetine-P450 complex, as shown in Figure 7. Analysis of this plot indicated that P450 and paroxetine-P450 complex attained equilibrium and oscillated around the average value after about 3 ns and remains stable to

the end of simulation. Consequently, this RMSD protein backbone pattern reflects stability and equilibrium during the course of simulation time (between 3 and 10 ns). Reduced values of RMSD of paroxetine-P450 complex infers that the binding of paroxetine to P450 lowers the protein movement degrees of freedom.

Besides, the radius of gyration ( $R_g$ ) values of free P450 and paroxetine-P450 complex was calculated as a function of time, as represented in Figure 8. The  $R_g$  values outline the protein's compactness with protein folding and unfolding along the 10 ns of MD simulations through thermodynamic basis. Initially, the  $R_g$  value was 2.28 nm then its value was stabilized at approximately 3000 ps, indicating that equilibrium was achieved after this time, as represented in Figure 8. The compactness of P450 structure during the simulation was estimated from the decreasing in the radius of gyration for backbone atoms. Moreover, Figure 8 implies that  $R_g$  assessment of P450 is not altered by the complexation with paroxetine. This indicates that the environment of P450 is not changed during the interaction with paroxetine. In addition, the total solvent accessible surface area (SAS) was evaluated for P450 in its native form and liganded form during 10 ns MD simulations as seen in Figure 9. Interestingly, the divergence profile of SAS in free P450 and P450-drug complex is similar to the change in  $R_g$  values, this resemblance asserts the precision of the results of the MD simulations.

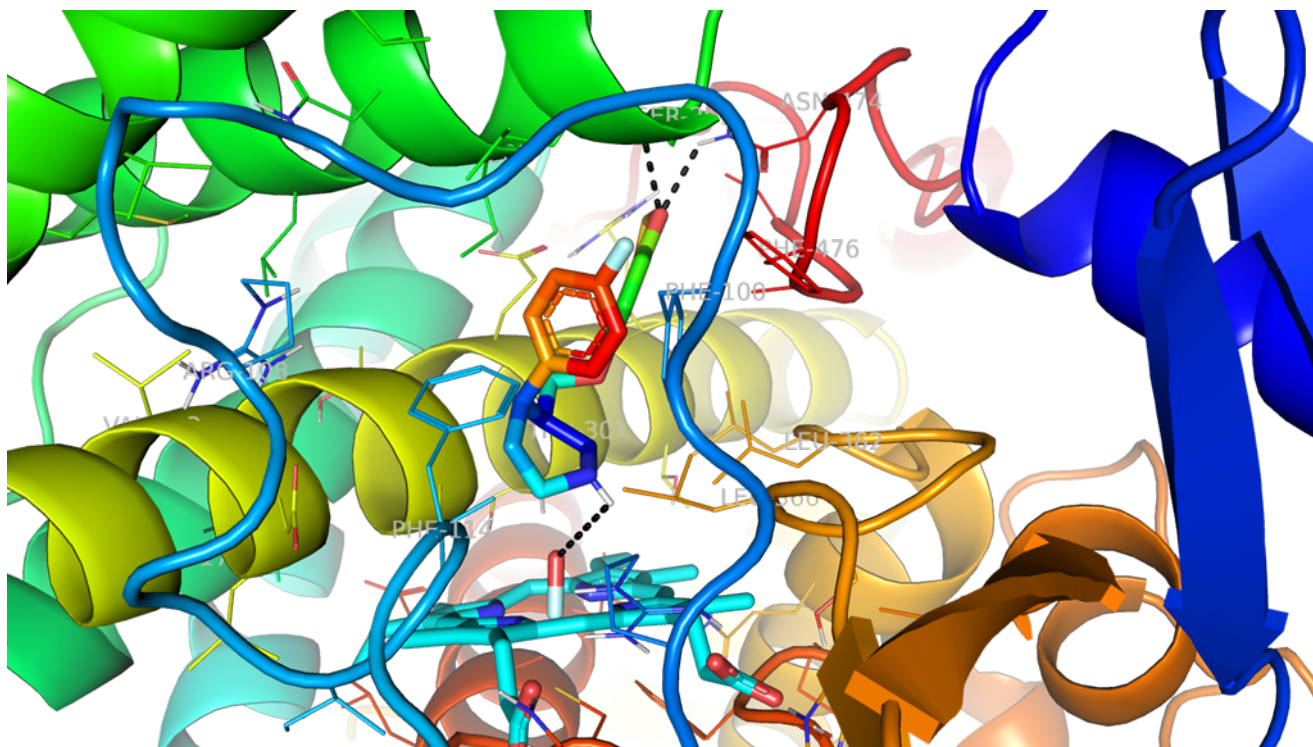


Figure 4. Binding site of paroxetine with P450. Paroxetine and P450's active site are shown as tube model, while Residues are shown as stick model.



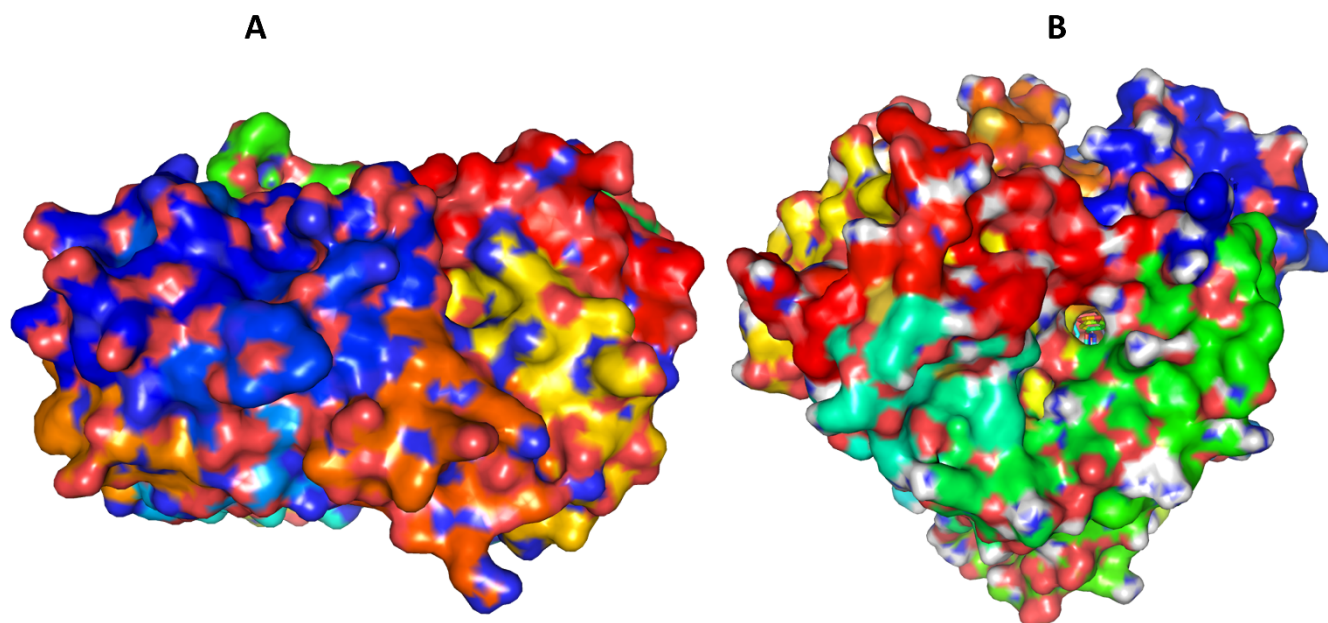


Figure 5. Surface representation of the native P450 (A) and paroxetine bound P450 (B) structures.

An elaborate assessment of the RMSF behavior of native P450 and P450 bound complex was carried out and the analyzed results represent the fluctuations of amino acids in free and catalyzed sites (Figure 10). This plot was recorded as against residue number based on 10 ns trajectory. The obtained RMSF profile manifests fluctuations at the catalytic site of P450 in the range of 0.05 to 0.47 nm. As shown in Figure 10, no significant fluctuations were disclosed at paroxetine binding site in the paroxetine-P450 complex compared to the free P450 protein. Thus, the obtained data clearly lead to the conclusion that residues at the internal cavity displayed low fluctuations for the drug, and paroxetine binding cavity architecture is nearly stick around its rigidity disposal during the 10 ns MD simulations.

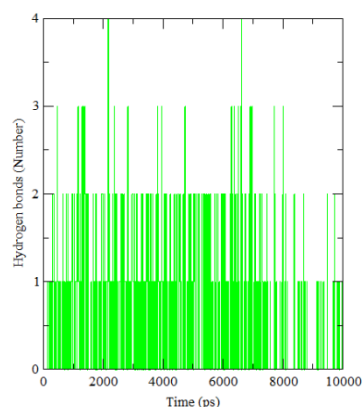


Figure 6. Total hydrogen bond intensity after 10 ns MD simulations for the Paroxetine-P450 complex.

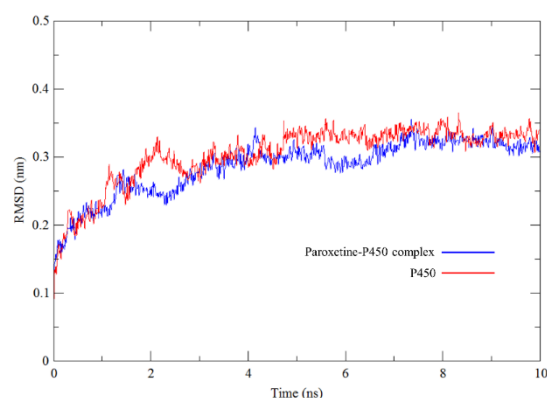


Figure 7. Backbone RMSD values of P450 and Paroxetine-P450 complex during 10 ns MD simulation.

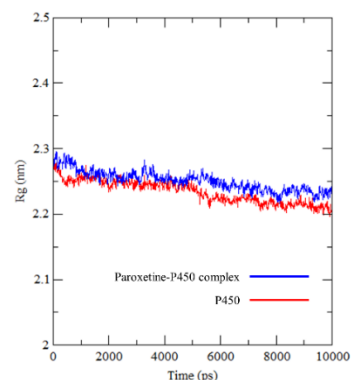


Figure 8. Radius of gyration (Rg) of the backbone of P450 and Paroxetine-P450 complex during 10 ns MD simulation.

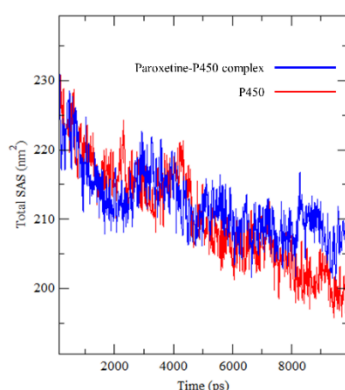


Figure 9. Total solvent accessible surface (SAS) of P450 and Paroxetine-P450 complex during 10 ns MD simulation.

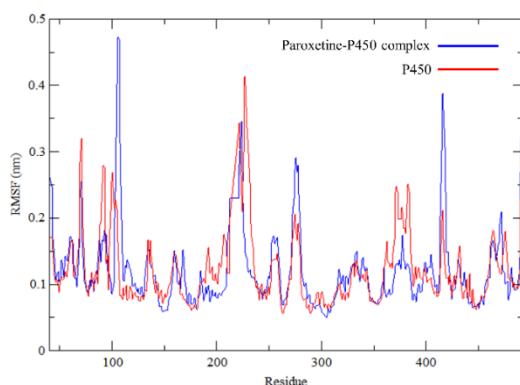


Figure 10. Root mean square fluctuation (RMSF) values of P450 and Paroxetine-P450 complex during 10 ns MD simulation.

## Conclusion

In conclusion, we have performed intensive computational analysis to figure out how paroxetine act as potent P450 inhibitor in its MBI. Our calculations provide several new insights. The possible mechanisms for the MBI of P450 by paroxetine involve C-H hydroxylation and N-hydroxylation at two different active sites on paroxetine structure. Both mechanisms are likely to occur indicating the potency of paroxetine as P450 inhibitor. Docking and MD simulations were carried out to inspect structural features and binding mechanisms. Docking analysis revealed the activity of paroxetine against P450 by the formation of polar bonds and  $\pi$ - $\pi$  interactions with phenylalanine residues. One polar bond was detected against the oxo moiety of the heme. This information is of particular interest since its good agreement with our DFT study. The result of docking was utilized for MD simulations which uncover valuable information to detect the effect of paroxetine binding on P450's conformational variation and the stability of paroxetine-P450 complex in aqueous medium. MD simulations studies revealed the stabilization of protein and protein-drug complexes at around 3000 ps. Also, the similarity of free P450 and the complex's atomic fluctuations scheme suggests the rigidity of the paroxetine-binding site nature during the 10 ns MD simulations.  $R_g$  values reflect the stability of the complex and that the conformation has not altered relative to P450's conformation.

## Experimental Section

### DFT studies

DFT calculations in this work were performed by using Gaussian 09<sup>[33]</sup> package for the mechanisms represented in scheme 2. The active site of P450 (Cpd I) was modeled as oxo-ferryl porphyrin species<sup>[25, 28b, 34]</sup>  $\text{Fe}^{4+}\text{O}^{2-}(\text{C}_{20}\text{N}_4\text{H}_{12})^-(\text{SH})^-$ . Full geometry optimizations for all species in doublet and quartet states were employed using the unrestricted B3LYP<sup>[35]</sup> functional in combination with the double- $\zeta$  LANL2DZ basis set for iron and 6-31G\* basis set for the other atoms, denoted BS1. Frequency calculations were also performed at the same level to depict the stationary points, obtain zero-point energy (ZPE), to calculate free energy, to evaluate the imaginary frequency for the transition states and to assure that ground states having no imaginary frequency. Thereafter, single-point energy calculations were carried out with the LANL2DZ (F) (Fe)/6-311+G\*\* (H,C,N,O,S) basis set (denoted BS2) in gas phase ( $\epsilon=1$ ) and in chlorobenzene solvent ( $\epsilon=5.7$ ) to mimic the bulk polarity influence of the protein environment<sup>[29, 36]</sup>, for the solvation effect, the self-consistent reaction field (SCRF) method was employed using the polarizable continuum model (PCM) solvation method<sup>[37]</sup>. In addition to, IRC calculations were also performed for several transition states to depict their pathways<sup>[38]</sup>.

### Molecular Docking

Molecular docking investigation was performed by using Autodock Tools (ADT) v1.5.6 and AutoDock Vina software<sup>[39]</sup>. Results were analyzed and visualized by using PyMOL v2.3.2. The crystallized three-dimensional structure of cytochrome P450 (PDB ID: 3NV5, 2.4 Å resolution) was obtained from Protein Data Bank (PDB). Missing residues in the crystal structure of 3NV5 were added using MODELLER 9.22<sup>[40]</sup> by the guidance of the 3NV6 (PDB ID) crystal structure. The Gaussian 09 package<sup>[33]</sup> optimized structure of the paroxetine at the B3LYP level<sup>[35b-d]</sup> with the 6-311G (d, p) basis set<sup>[41]</sup> was used as initial structures for docking and MD simulations. Paroxetine was docked at various sites in the access channel of P450. Macromolecules were visualized and separated from ligand, solvent and unneeded residues by using UCSF Chimera<sup>[42]</sup>. Isolated protein receptor was prepared for docking by optimization by means of ADT, this optimization includes addition of polar hydrogens and setting the grid box according to the best configuration of the active site amino acid residues<sup>[43]</sup>.

### Molecular dynamics simulations

The complex of paroxetine (PDB ID: 3NV5) with the lowest binding free energy was selected for MD simulation. Water molecules were stripped out from paroxetine-P450 complex. The Dundee PRODRG 2.5 server was utilized to build the starting topology parameters of the paroxetine<sup>[44]</sup>, these parameters were implanted into the topology parameters of the enzyme. The 10 ns MD simulations of P450 and paroxetine-P450 complexes were carried out using GROMACS 2019.4 software packages<sup>[45]</sup> with the GROMOS9643a1 force field<sup>[46]</sup>. The enzyme and drugs-enzyme complexes were placed in a dodecahedron box with the periodic boundary conditions, the box volume was 591.64 nm<sup>3</sup>. The simple point charge (SPC) water model was employed and three chloride counter-ions were added to attain electroneutrality<sup>[47]</sup>. The steepest descent energy minimization method was used for 10 ps to relieve the thermodynamically less favorable interactions<sup>[48]</sup>. Thereafter, systems were equilibrated on two stages at a temperature of 300 K for 100 ps each; NVT and NPT ensembles<sup>[49]</sup>. Finally, the 10 ns MD simulation was executed at 300 K temperature and 1 bar pressure. The long-range electrostatic terms were contained using the particle mesh Ewald algorithm<sup>[50]</sup>, and the motion equations were employed by applying the leap-frog integrator with the time-step of 2 fs. Trajectories were visualized using VMD<sup>[51]</sup> and UCSF Chimera and images were generated using UCSF Chimera<sup>[42]</sup> and PyMOL v2.3.2.

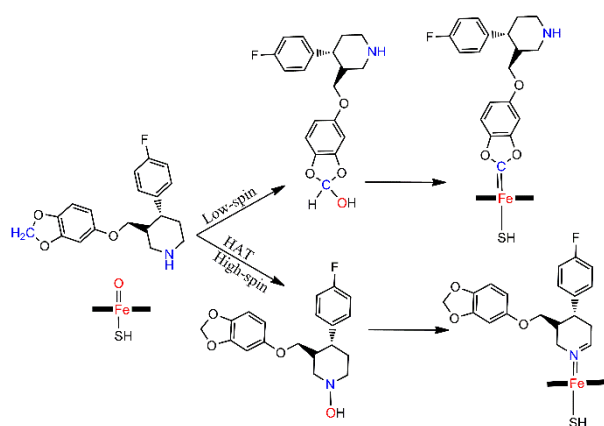
## Acknowledgements

This work has DGI Projects no. CTQ2015-63997-C2, Authors also thank the Centro de Computación Científica of the UAM for the generous support and computing time.

**Keywords** Cytochrome P450 • Paroxetine • Catalyzed biotransformation • Mechanism-based inactivation • Reaction mechanism

- [1] D. W. Nebert and T. P. Dalton, *Nature reviews. Cancer* **2006**, 6, 947.
- [2] M. Sono, M. P. Roach, E. D. Coulter and J. H. Dawson, *Chemical Reviews* **1996**, 96, 2841-2888.
- [3] a) L. P. Wackett, M. J. Sadowsky, L. M. Newman, H.-G. Hur and S. Li, *Nature* **1994**, 368, 627-629; b) C. Duport, R. Spagnoli, E. Degryse and D. Pompon, *Nature biotechnology* **1998**, 16, 186-189.
- [4] M. A. Correia and P. R. O. de Montellano in *Inhibition of cytochrome P450 enzymes*, Springer, **2005**, pp. 247-322.
- [5] S. Nagano, H. Li, H. Shimizu, C. Nishida, H. Ogura, P. R. O. de Montellano and T. L. Poulos, *Journal of Biological Chemistry* **2003**, 278, 44886-44893.
- [6] a) P. R. O. De Montellano, *Cytochrome P450: structure, mechanism, and biochemistry*, Springer Science & Business Media, **2005**, p; b) A. Rodrigues, D. Fernandez, M. Nosarzewski, W. Pierce Jr and R. Prough, *Chemical research in toxicology* **1991**, 4, 281-289.
- [7] a) M. Murray and G. F. Reidy, *Pharmacol Rev* **1990**, 42, 85-101; b) S. Rendic and F. J. D. Carlo, *Drug metabolism reviews* **1997**, 29, 413-580; c) U. M. Kent, M. Jushchshyn and P. F. Hollenberg, *Current drug metabolism* **2001**, 2, 215-243.
- [8] P. Chuanprasit, S. H. Goh and H. Hirao, *ACS Catalysis* **2015**, 5, 2952-2960.
- [9] H. Hirao, Z. H. Cheong and X. Wang, *The Journal of Physical Chemistry B* **2012**, 116, 7787-7794.
- [10] S. Shaik, S. Cohen, Y. Wang, H. Chen, D. Kumar and W. Thiel, *Chemical reviews* **2009**, 110, 949-1017.
- [11] K. Brøsen, L. F. Gram and P. Kragh-Sørensen, *Therapeutic drug monitoring* **1991**, 13, 177-182.
- [12] S. Laugesen, T. P. Enggaard, R. S. Pedersen, S. H. Sindrup and K. Brøsen, *Clinical Pharmacology & Therapeutics* **2005**, 77, 312-323.
- [13] B. G. Pollock, *Am J Psychiatry* **1996**, 1, 53.
- [14] R. R. Naik, N. S. Gandhi, M. Thakur and V. Nanda, *Food chemistry* **2019**, 125182.
- [15] S. Gharaghani, T. Khayamian and F. J. S. C. Keshavarz, **2012**, 23, 341-350.
- [16] S. K. Lüdemann, V. Lounnas and R. C. J. J. o. m. b. Wade, **2000**, 303, 797-811.
- [17] a) S. Shaik, D. Kumar and S. P. de Visser, *Journal of the American Chemical Society* **2008**, 130, 14016-14016; b) F. Ogliaro, N. Harris, S. Cohen, M. Filatov, S. P. de Visser and S. Shaik, *Journal of the American Chemical Society* **2000**, 122, 8977-8989; c) C. Li, W. Wu, D. Kumar and S. Shaik, *Journal of the American Chemical Society* **2006**, 128, 394-395.
- [18] a) S. P. de Visser, F. Ogliaro and S. Shaik, *Angewandte Chemie* **2001**, 113, 2955-2958; b) S. P. de Visser, F. Ogliaro, N. Harris and S. Shaik, *Journal of the American Chemical Society* **2001**, 123, 3037-3047; c) D. Kumar, B. Karamzadeh, G. N. Sastry and S. P. de Visser, *Journal of the American Chemical Society* **2010**, 132, 7656-7667.
- [19] a) C. Li, L. Zhang, C. Zhang, H. Hirao, W. Wu and S. Shaik, *Angewandte Chemie International Edition* **2007**, 46, 8168-8170; b) P. Rydberg, U. Ryde and L. Olsen, *Journal of chemical theory and computation* **2008**, 4, 1369-1377; c) C. Li, W. Wu, K. B. Cho and S. Shaik, *Chemistry-A European Journal* **2009**, 15, 8492-8503; d) S. Shaik, Y. Wang, H. Chen, J. Song and R. Meir, *Faraday Discussions* **2010**, 145, 49-70.
- [20] J. T. Groves and D. V. Adhyam, *Journal of the American Chemical Society* **1984**, 106, 2177-2181.
- [21] F. P. Guengerich, *The AAPS journal* **2006**, 8, E101-E111.
- [22] P. Rydberg and L. Olsen, *Journal of chemical theory and computation* **2011**, 7, 3399-3404.
- [23] L. Ji and G. Schüürmann, *Angewandte Chemie International Edition* **2013**, 52, 744-748.
- [24] L. Ji and G. Schüürmann, *Chemical research in toxicology* **2015**, 28, 585-596.
- [25] S. P. de Visser, F. Ogliaro, P. K. Sharma and S. Shaik, *Journal of the American Chemical Society* **2002**, 124, 11809-11826.
- [26] P. R. O. de Montellano and J. J. De Voss in *Substrate oxidation by cytochrome P450 enzymes*, Springer, **2005**, pp. 183-245.
- [27] Y. Wang, D. Kumar, C. Yang, K. Han and S. Shaik, *The Journal of Physical Chemistry B* **2007**, 111, 7700-7710.
- [28] a) H. Basch, K. Mogi, D. G. Musaev and K. Morokuma, *Journal of the American Chemical Society* **1999**, 121, 7249-7256; b) F. Ogliaro, N. Harris, S. Cohen, M. Filatov, S. P. de Visser and S. Shaik, *Journal of the American Chemical Society* **2000**, 122, 8977-8989.
- [29] L. Ji and G. Schüürmann, *The Journal of Physical Chemistry B* **2012**, 116, 903-912.
- [30] S. Shaik, D. Kumar, S. P. de Visser, A. Altun and W. Thiel, *Chemical reviews* **2005**, 105, 2279-2328.
- [31] S. T. Seger, P. Rydberg and L. Olsen, *Chemical research in toxicology* **2015**, 28, 597-603.
- [32] C. A. Hunter, J. Singh and J. M. J. J. o. m. b. Thornton, **1991**, 218, 837-846.
- [33] M. J. Frisch, G. W. Trucks, H. B. Schlegel, G. E. Scuseria, M. A. Robb, J. R. Cheeseman, G. Scalmani, V. Barone, B. Mennucci, G. A. Petersson, H. Nakatsuji, M. Caricato, X. Li, H. P. Hratchian, A. F. Izmaylov, J. Bloino, G. Zheng, J. L. Sonnenberg, M. Hada, M. Ehara, K. Toyota, R. Fukuda, J. Hasegawa, M. Ishida, T. Nakajima, Y. Honda, O. Kitao, H. Nakai, T. Vreven, J. A. Montgomery Jr., J. E. Peralta, F. Ogliaro, M. J. Bearpark, J. Heyd, E. N. Brothers, K. N. Kudin, V. N. Staroverov, R. Kobayashi, J. Normand, K. Raghavachari, A. P. Rendell, J. C. Burant, S. S. Iyengar, J. Tomasi, M. Cossi, N. Rega, N. J. Millam, M. Klene, J. E. Knox, J. B. Cross, V. Bakken, C. Adamo, J. Jaramillo, R. Gomperts, R. E. Stratmann, O. Yazyev, A. J. Austin, R. Cammi, C. Pomelli, J. W. Ochterski, R. L. Martin, K. Morokuma, V. G. Zakrzewski, G. A. Voth, P. Salvador, J. J. Dannenberg, S. Dapprich, A. D. Daniels, Ö. Farkas, J. B. Foresman, J. V. Ortiz, J. Cioslowski and D. J. Fox, *Wallingford, CT* **2009**.
- [34] C. Li, W. Wu, K. B. Cho and S. Shaik, *Chemistry-A European Journal* **2009**, 15, 8492-8503.
- [35] a) A. D. Becke, *The Journal of chemical physics* **1992**, 96, 2155-2160; b) A. D. Becke, *The Journal of Chemical Physics* **1993**, 98, 5648-5652; c) A. D. Becke, *Physical review A* **1988**, 38, 3098; d) C. Lee, W. Yang and R. G. Parr, *Physical review B* **1988**, 37, 785.
- [36] a) B. Honig and A. Nicholls, *Science* **1995**, 268, 1144-1149; b) C. N. Schutz and A. Warshel, *Proteins: Structure, Function, and Bioinformatics* **2001**, 44, 400-417.
- [37] a) S. Miertuš, E. Scrocco and J. Tomasi, *Chemical Physics* **1981**, 55, 117-129; b) J. Tomasi, B. Mennucci and R. Cammi, *Chemical reviews* **2005**, 105, 2999-3094.
- [38] K. Fukui in *The path of chemical reactions—the IRC approach*, World Scientific, **1997**, pp. 471-476.
- [39] O. Trott and A. J. Olson, *Journal of computational chemistry* **2010**, 31, 455-461.
- [40] A. Šali and T. L. J. J. o. m. b. Blundell, **1993**, 234, 779-815.
- [41] W. J. Hehre, L. Radom, P. v. R. Schleyer and J. A. Pople, *Ab initio molecular orbital theory*, Wiley New York et al., **1986**, p.
- [42] E. F. Pettersen, T. D. Goddard, C. C. Huang, G. S. Couch, D. M. Greenblatt, E. C. Meng and T. E. Ferrin, *Journal of computational chemistry* **2004**, 25, 1605-1612.
- [43] R. T. Nolte, G. B. Wisely, S. Westin, J. E. Cobb, M. H. Lambert, R. Kurokawa, M. G. Rosenfeld, T. M. Willson, C. K. Glass and M. V. Milburn, *Nature* **1998**, 395, 137.
- [44] A. W. Schüttelkopf and D. M. Van Aalten, *Acta Crystallographica Section D: Biological Crystallography* **2004**, 60, 1355-1363.
- [45] a) H. J. Berendsen, D. van der Spoel and R. van Drunen, *Computer physics communications* **1995**, 91, 43-56; b) E. Lindahl, B. Hess and D. Van Der Spoel, *Molecular modeling annual* **2001**, 7, 306-317.
- [46] W. F. van Gunsteren, S. Billeter, A. Eising, P. Hünenberger, P. Krüger, A. Mark, W. Scott and I. Tironi, *Vdf Hochschulverlag AG an der ETH Zürich, Zürich* **1996**, 86.
- [47] H. Berendsen, J. Postma and W. Van Gunsteren in *J. Hermans in Intermolecular Forces, Vol. Reidel, Dordrecht*, **1981**.
- [48] B. Hess, C. Kutzner, D. Van Der Spoel and E. Lindahl, *Journal of chemical theory and computation* **2008**, 4, 435-447.
- [49] M. Parrinello and A. Rahman, *Journal of Applied physics* **1981**, 52, 7182-7190.
- [50] a) T. Darden, D. York and L. Pedersen, *The Journal of chemical physics* **1993**, 98, 10089-10092; b) U. Essmann, L. Perera, M. L. Berkowitz, T. Darden, H. Lee and L. G. Pedersen, *The Journal of chemical physics* **1995**, 103, 8577-8593.
- [51] W. Humphrey, A. Dalke and K. Schulten in *VMD-Visual Molecular Dynamics J Mol Graph* **14: 33-38, Vol. 1996**.

## Entry for the Table of Contents



Why paroxetine is a potent cytochrome P450 inhibitor? DFT studies on the mechanism-based inactivation of P450 revealed the availability of two active sites on the structure of paroxetine vulnerable to hydroxylation by P450. the mechanisms of dehydration and coordination to heme of hydroxylated paroxetine, docking analysis and MD simulations confirmed the compatibility and potency of paroxetine as P450' inhibitor.